

Influence of oxygen supply rates on performances of catalytic membrane reactors

Application to the oxidative coupling of methane

Stéphane Haag, Andre C. van Veen*, Claude Mirodatos

*Institut de Recherches sur la Catalyse et l'Environnement de LYON, UMR 5256 (CNRS/Université Claude Bernard Lyon 1),
2 avenue Albert Einstein, 69626 Villeurbanne Cédex, France*

Available online 28 June 2007

Abstract

The impact of oxygen permeability using an ionic oxygen conducting membrane reactor with surface catalyst was investigated for the oxidative coupling of methane to higher hydrocarbons. Dense $\text{Ba}_{0.5}\text{Sr}_{0.5}\text{Co}_{0.8}\text{Fe}_{0.2}\text{O}_{3-\delta}$ (BSCFO), $\text{Ba}_{0.5}\text{Sr}_{0.5}\text{Mn}_{0.8}\text{Fe}_{0.2}\text{O}_{3-\delta}$ (BSMFO) and $\text{BaBi}_{0.4}\text{Fe}_{0.6}\text{O}_3$ (BBFO) membrane disks with Pt/MgO catalysts were prepared by sol–gel deposition or wash-coating. It is demonstrated that the oxygen supply by permeation needs to fit to the consumption during the coupling reaction. In case of insufficient oxygen supply comparably poor conversions are observed while higher oxygen fluxes lead to increased methane conversions, especially in the presence of an efficient catalyst. Generally, increasing catalytic activity leads to lower C_2 selectivity, especially for low oxygen permeation fluxes. The concept of a reactor employing dense catalytic membranes is viable, but the present study identifies further potential when the activity of the catalyst for the oxidative coupling is improved, leading to an overall enhanced performance of the membrane reactor.

© 2007 Elsevier B.V. All rights reserved.

Keywords: Dense membrane; Perovskite; Platinum; MgO; Oxygen permeability

1. Introduction

The valorization of natural gas is a domain of permanent research but nowadays renewed interest for routes, which were practically abandoned in this area, emerged again due to the recent high oil prices. Thus, the abundant resources of natural gas available at still reasonable prices and foreseeable future shortage of petroleum have reactivated research on the oxidative coupling of methane (OCM) yielding ethane and ethylene, as value-added and easy to liquefy products. Nevertheless, operating conditions are difficult to optimize because C_2 products (C_2H_4 and C_2H_6) are more reactive than the reactant (CH_4) [1]. Typically, the higher the methane conversion, the lower the C_2 selectivity is. It has been estimated in previous literature studies assuming lower oil prices that a single-pass conversion of 35–37% and selectivity of

88–85%, equivalent to a C_2 yield of 30+%, is required to attain commercial competitiveness for OCM [2]. In fact, results obtained are still far away from this expectation while the limit of the C_2 yield in a fixed bed reactor is found to be around 25% [3,4]. Despite extensive research efforts in the past considering mainly process concepts based on fixed bed reactors, alternative reactor concepts with inherent need for adapted catalysts have to be invented. One of the most promising design solutions could be catalytic membrane reactors allowing a cost cutting use of air instead of oxygen and possibly higher productivity as flammability issues of the reactant mixture close to stoichiometry could be avoided.

Inorganic membranes for gas separation can be divided in two classes: porous and dense membranes. Porous membranes exhibit high permeability combined with relatively low selectivity. On the other hand, dense membranes show much better selectivity but lower permeability than porous membranes. Within the category of dense membranes, ionic oxygen conducting membranes (IOCM) offer the unique advantage to provide activated oxygen at its surface while preventing hydrocarbon losses to the opposite side.

* Corresponding author at: Université de Lyon, Institut de Recherches sur la Catalyse et l'Environnement de LYON (IRCELYON), UMR 5256 (CNRS/Université Claude Bernard Lyon 1), 2 avenue Albert Einstein, 69626 Villeurbanne Cédex, France. Tel.: +33 472 44 5482; fax: +33 472 44 5300.

E-mail address: vanveen@ircelyon.univ-lyon1.fr (A.C. van Veen).

First published works [5] in the domain of OCM used either porous membranes combined with catalysts in form of a fixed bed [6,7] or dense membranes without catalysts. In the former case, the porous membrane was used only as a gaseous oxygen distributor along the catalyst bed, without significant yield improvement. In the latter case, all attempts suffer from comparably low productivity [2,8–13]. Previous work in our group dedicated to oxidative dehydrogenation of ethane (ODHE) [14] indicated the interest to use an IOCM membrane feeding directly a layered catalyst on top of the membrane without passing oxygen via the gas-phase.

Mixed-conducting oxide membranes such as perovskite based systems are well known for their abilities to separate oxygen from air due to mobile oxygen defects in their lattice being only susceptible for oxygen transportation [15–21]. The performance of dense membranes can be affected by many structural factors such as grain size, e.g. altered by sintering conditions, membrane thickness and microstructure or bulk density. Furthermore, for temperatures at which those membranes are operating, the chemical potential gradient of oxygen and different membrane compositions can cause over magnitudes different oxygen permeation fluxes [15].

Among dense perovskite membranes, $\text{Ba}(\text{Co,Fe})\text{O}_{3-\delta}$ based perovskites such as $\text{Ba}_{0.5}\text{Sr}_{0.5}\text{Co}_{0.8}\text{Fe}_{0.2}\text{O}_{3-\delta}$, $\text{Ba}_{0.5}\text{Sr}_{0.5}\text{Co}_{0.6}\text{Fe}_{0.4}\text{O}_{3-\delta}$ or $\text{Ba}(\text{Co,Fe,Zr})\text{O}_{3-\delta}$ exhibit stable oxygen fluxes at high temperatures, in the presence of an air/He gradient of the oxygen chemical potential [22,23] and during a membrane reactor based partial oxidation of methane (POM) [24,25] or ODHE [14]. Shao et al. [26] studied the influence of the barium content in $\text{SrCo}_{0.8}\text{Fe}_{0.2}\text{O}_{3-\delta}$ and showed that the addition of barium results in higher oxygen permeability and lower activation energy for oxygen transportation at high temperature.

In this study, three kinds of perovskites membranes with different oxygen permeability were used to study the influence of oxygen supply rates on catalytic performance at given temperatures. Furthermore, the way to prepare the coated catalysts impacting on the intrinsic catalytic properties was altered in order to study at given oxygen supply the influence of the catalyst nature on the C_2 selectivity and the methane conversion during the reaction. It should be noted that the catalyst itself was not optimized, but specifically chosen for its thermal stability when operating at temperatures until 1000°C and the relative ease to deposit it on the membrane surface.

2. Experimental

2.1. Membrane materials

In this work, 1 mm thick dense $\text{Ba}_{0.5}\text{Sr}_{0.5}\text{Co}_{0.8}\text{Fe}_{0.2}\text{O}_{3-\delta}$ (BSCFO), $\text{Ba}_{0.5}\text{Sr}_{0.5}\text{Mn}_{0.8}\text{Fe}_{0.2}\text{O}_{3-\delta}$ (BSMFO) and $\text{BaBi}_{0.4}\text{Fe}_{0.6}\text{O}_3$ (BBFO) membrane disks were prepared with specific conditions of densification for each material.

The synthesis of the $\text{Ba}_{0.5}\text{Sr}_{0.5}\text{Co}_{0.8}\text{Fe}_{0.2}\text{O}_{3-\delta}$ (BSCFO) oxide proceeded by the so-called citrates method using citric acid and EDTA as complex formation agents [22] (EDTA was used to dissolve the barium nitrate). Citric acid was added in 1:1 molar ratio with respect to the sum of metal salts. The resulting

powder was calcined in air at 900°C for 4 h. Recently we added a novel step conditioning the perovskite powders by ball milling in *iso*-propanol suspension, improving the material properties of the final disks in terms of bulk density and mechanical stability. The beneficial effect is related to a decreased grain size obtained prior to pelletizing. Then, the membrane was prepared by isostatic pressing with a pressure of 220 MPa applied for 2 min to the powder. Results showed that ~ 0.5 g of powder yielded a black colored, 1 mm thick, 15 mm-diameter disk. Densification of the disk was achieved by sintering in air for 8 h at 1160°C with a heating and cooling ramp of $2^\circ\text{C}/\text{min}$. The final diameter of the disk was decreased to 13 mm by shrinkage during sintering.

The preparation of the BSMFO membranes followed comparable steps as those ones outlined for the BSCFO membrane. The powder was calcined in air at 1200°C for 4 h. Then, the sintering of the disk was performed at 1240°C for 8 h ($2^\circ\text{C}/\text{min}$ ramps) and its diameter after densification was 15 mm. On the other hand, the BBFO powder obtained by the citrates method was calcined at 900°C for 4 h. The sintering of the membrane proceeded at 1000°C for 8 h ($2^\circ\text{C}/\text{min}$ ramp) and the diameter of the disk after densification was also 15 mm.

2.2. Membrane characterization

Formation of the perovskite structure was checked by X-ray diffraction (Fig. 1), using a Bruker D5005 system in the 2θ range $3\text{--}80^\circ$, a step width of 0.02° and a counting time of 1 s and $\text{Cu K}_{\alpha 1+\alpha 2}$ radiation (1.54184 \AA). The microstructure of the membranes was observed by scanning electron microscopy (Fig. 2).

2.3. Membrane surface modification

In our previous work [14], parameters for a model describing the oxygen permeation through the BSCFO membrane were determined and the modeling study underlined the importance of surface exchange processes for oxygen permeation. This modeling approach was confirmed by experiments carried out under permeation conditions, showing that oxygen fluxes were

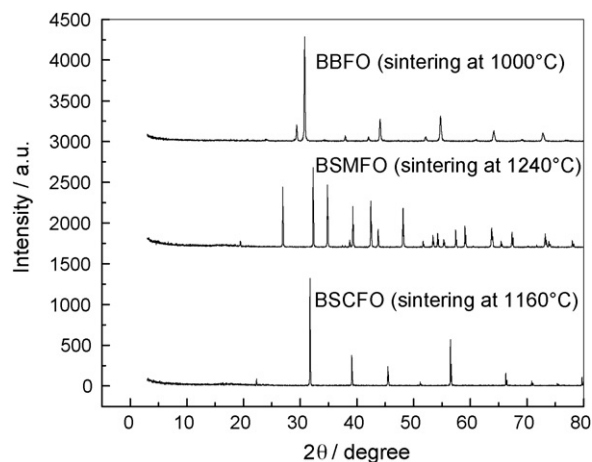


Fig. 1. XRD patterns of perovskite membranes after densification.

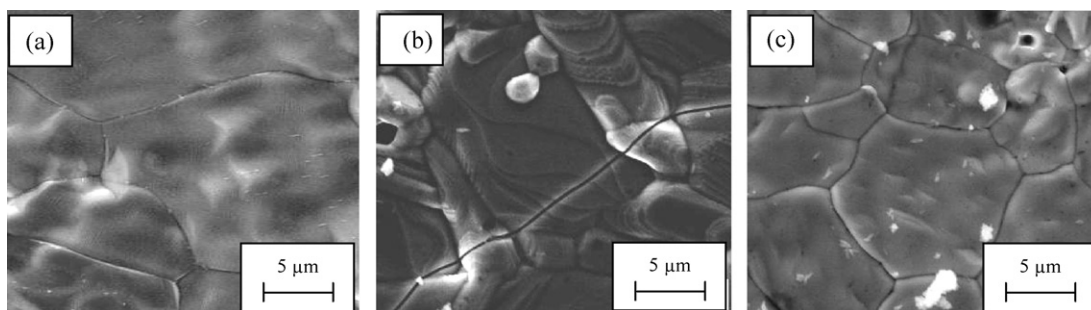


Fig. 2. Microstructure of BSCFO (a), BSMFO (b) and BBFO (c) membranes after densification.

enlarged by a factor of about two depositing a V/MgO layer on the membrane surface. Thus, the interest of catalytic surface modifications was demonstrated for the case where processes at the surface of the hydrocarbon rich side affect the overall membrane performance. Obviously, this is the case even for the simple oxygen permeation.

In the present study, the membrane surface was modified with catalytic layers to improve the efficiency of the membrane reactor, i.e. to enhance C_2 selectively and methane conversion. MgO was chosen as support and platinum was selected as active species. Magnesium oxide is one of the well known catalyst supports for the OCM reaction showing high thermal stability, required basicity and no deep reducibility under the operating conditions. In general, MgO is associated to lithium, given the fact that Li/MgO is a reference OCM system for reasonable C_2 selectivity [27–30]. However, membranes require high operating temperatures to provide adapted oxygen permeability and due to its high volatility under those conditions ($800\text{ }^\circ\text{C} < T < 1000\text{ }^\circ\text{C}$), lithium was excluded as modifier in this study. In turn, considering stable alternatives, platinum which is much more resistant to high temperature and is known to easily activate methane in POM was selected [31,32].

Two routes were tested for the deposition of the oxide, a sol–gel and a wash-coating method, followed by calcination at $800\text{ }^\circ\text{C}$. However, a good adhesion of the catalyst on the membrane surface depends highly on the weight of catalyst deposited on the surface. Scanning electron microscopy (Fig. 3a) revealed that about half of the membrane surface is coated by the magnesium oxide using the sol–gel method. Even at a one magnitude lower magnification it can be observed that the sol–gel method yields a non-uniform deposition of the catalyst while the layer deposited with a

wash coat method covers the whole surface uniformly (Fig. 3b).

Platinum was added by impregnation, using tetraammine platinum(II) nitrate as metal precursor (Sigma–Aldrich). The estimated loading of Pt was about 2% on the MgO support. The maximum gain in weight after deposition of the Pt/MgO catalyst was about 2.75 times higher with the wash-coat method ($\sim 7.7\text{ mg}$) compared to the sol–gel method ($\sim 2.8\text{ mg}$). A higher catalyst loading with good adherence was not feasible as the Pt/MgO layer detached from the membrane surface at high temperature.

2.4. Oxygen permeability

Information on oxygen permeability, key property of mixed conducting membranes, was acquired in the temperature range of $800\text{--}1000\text{ }^\circ\text{C}$. An O_2/N_2 mixture presenting reconstituted air was fed to the oxygen-rich membrane compartment, while helium was used as a sweep gas on the permeate side. The membrane disk (about 1 mm thick) was sealed with gold rings in between two dense alumina tubes (outer diameter: 12 mm, inner diameter: 8 mm) by heating to $900\text{ }^\circ\text{C}$ for 48 h. The total pressure at the oxygen-rich side was adjusted to 1.1 bar for a constant total flow rate of the mixed O_2 and N_2 streams controlled by mass flow controllers. Gas chromatography (HP 5890 Series II, 13X packed column) allowed complete analysis of gases at both sides of the membrane.

2.5. Catalytic membrane reactors

The experimental device for catalytic tests is depicted in Fig. 4. The air feed supplied the mixed conducting membrane

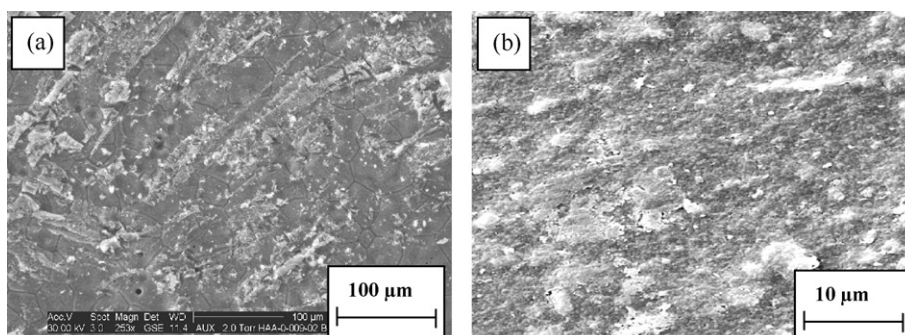


Fig. 3. SEM image of a surface modified BSCFO membrane by a sol–gel method (a, left) and by a wash-coat method (b, right).

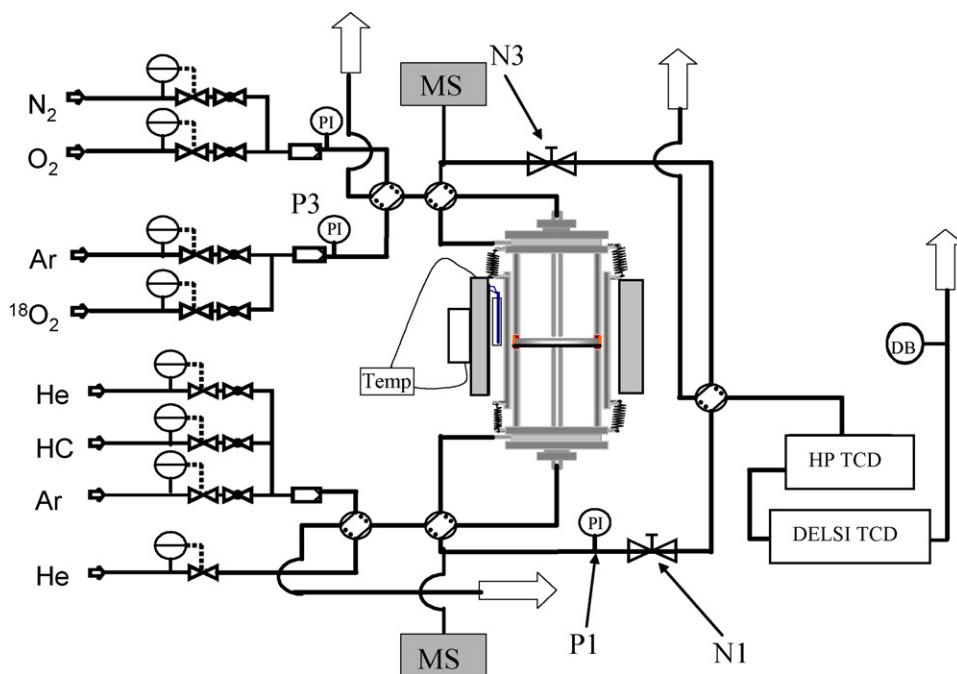


Fig. 4. Experimental device for catalytic tests.

with oxygen allowing the dense perovskite membrane to provide activated oxygen for the OCM. Mass flow controllers adjusted the flow rates of helium used as carrier gas and methane on the reactant side. Two gas chromatographs (TCDs) were used to analyze all gases. The CH_4/He mixture flow rate was fixed to 85 mL min^{-1} and the reconstituted air flow rate was set to 100 mL min^{-1} . The methane concentration in the reactant flow was fixed at 10%. Experiments were conducted in a temperature range of $800\text{--}1000^\circ\text{C}$ due to the comparably low oxygen permeability for some of the selected perovskites and a lack of activity for the non-optimized Pt/MgO catalyst at lower temperatures.

3. Results and discussion

3.1. Oxygen permeability for bare membranes

From a mechanistic point of view, the oxygen permeation through a dense membrane from the oxygen rich compartment (A) to the permeate compartment (B) of the membrane can be subdivided into the following steps:

- oxygen transport from the bulk gas phase to the surface of the side A;
- surface activation of oxygen and integration into oxygen vacancies (adsorption);
- ionic oxygen bulk diffusion and the diffusion of electrically charged species;
- surface release causing desorption of oxygen;
- diffusion of molecular oxygen from the B side surface to the gas volume.

Generally, each of these steps has a different frequency factor and activation energy and could be rate limiting

according to the reactor design, mode of operation, properties of the membrane material and eventually surface catalyst. Previous work [14] indicated also that the rate limiting step may change according to the temperature range investigated. The permeability of the three tested membranes and an estimation of the activation energy are presented in Table 1.

3.1.1. BSCFO membrane

For the $\text{Ba}_{0.5}\text{Sr}_{0.5}\text{Co}_{0.8}\text{Fe}_{0.2}\text{O}_{3-\delta}$ membrane the oxygen fluxes for the activated permeation process and an estimation of the activation energy indicated a change in the rate determining step at around 725°C : for $T < 725^\circ\text{C}$, the permeation of the oxygen is limited by surface steps and for $T > 725^\circ\text{C}$, the diffusion through the bulk becomes the rate limiting step.

3.1.2. BBFO membrane

In the case of the BBFO membrane [33], oxygen permeation fluxes are significantly lower than those obtained for the BSCFO membrane and are comparable to values reported in literature for a $\text{La}_{0.6}\text{Sr}_{0.4}\text{Co}_{0.6}\text{Fe}_{0.4}\text{O}_{3-\delta}$ membrane [11].

Table 1
Comparison of bare membranes permeability and estimation of activation energies

Membranes	Permeability ($\text{mL min}^{-1} \text{cm}^{-2}$) $T = 900^\circ\text{C}$	Activation energies (kJ mol^{-1})	
		E_a (high temperature)	E_a (low temperature)
BSCFO	1.51	46	84
BBFO	0.28	–	102
BSMFO	0.014	196	77

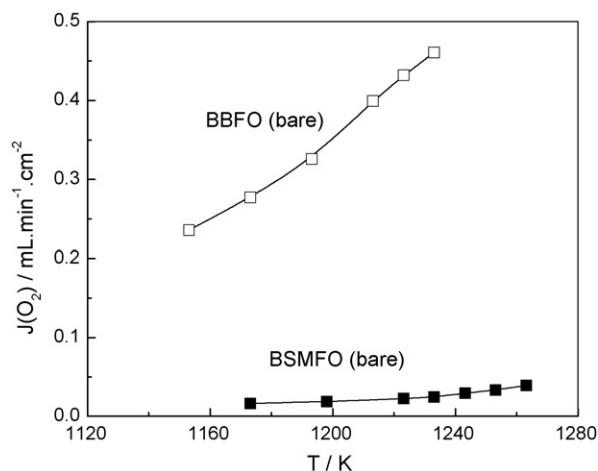


Fig. 5. Oxygen permeation for the BBFO and BSMFO membranes using a reconstituted air: 100 mL min⁻¹/He: 100 mL min⁻¹ gradient.

3.1.3. BSMFO membrane

The oxygen permeation flux of the BSMFO membrane increases with increasing temperature but to a much smaller extent compared to the former described membranes.

The oxygen permeation fluxes for the BSMFO and BBFO membranes are presented in Fig. 5 using a reconstituted air feed of 100 mL min⁻¹, while the He flow rate was 100 mL min⁻¹. The main drawback with the BBFO membrane is its lack of thermal stability. In fact, the membrane is not stable at temperatures above 960 °C and cracking or partial melting of the disk is observed increasing the temperature beyond that point. This is a substantial limitation for its utilization in a membrane reactor for the high temperature OCM reaction. The comparably high activation energy at high temperatures indicates that the oxygen diffusion through the bulk of the BSMFO membrane is much more difficult compared to the other perovskite samples. Indeed, Lu et al. [15] studied the oxygen permeability of Ba_{0.5}Sr_{0.5}Co₁Fe_{0.1}Mn_{0.1}O_{3-δ} membranes with M = Fe, Cr, Zr or Mn and it was demonstrated that the permeability increased in the following order Fe > Cr > Zr > Mn with a higher activation energy for the Ba_{0.5}Sr_{0.5}Co₁Fe_{0.1}Mn_{0.1}O_{3-δ} membrane compared to the other samples. This behavior could relate to the low oxygen mobility in the volume of the membrane hindered by the relatively small amount of vacancies present in the structure. However, further studies, e.g. the determination of the non-stoichiometry as a function of temperature, are required to confirm this assumption.

3.2. Oxygen permeability of the surface modified membranes

3.2.1. BSCFO membrane

Permeation tests were first performed with the BSCFO membranes wash-coated with Pt/MgO using a feed composed of a 100 mL min⁻¹ O₂/N₂ mixture and 50 mL min⁻¹ of He used as sweep gas on the permeate side and the results were compared to those obtained with the bare membrane (Fig. 6). Although oxygen fluxes were similar for the bare and the sol-

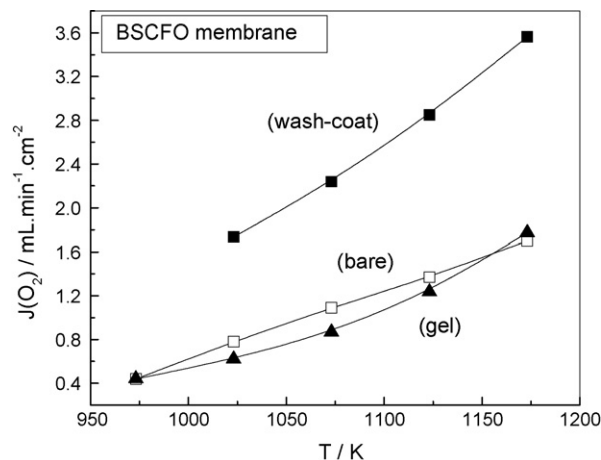


Fig. 6. Oxygen permeation through BSCFO based modified membranes (reconstituted air: 50 mL min⁻¹/He: 100 mL min⁻¹).

gel modified membranes, the wash-coat modified membrane showed an about 2.5 times higher oxygen permeability. From our previous works, this significant increase in oxygen permeability after surface modification can be assigned to oxygen desorption on the modified surface in the presence of the MgO layer. The behavior of the partially covered membrane could be related to readsorption effects where oxygen initially released from the MgO phase becomes captured by the bare BSCFO surface. The latter hypothesis is in agreement with the fact that a former kinetic study carried out in the Temporal analysis of products (TAP) fast pulsed reactor indicated a rapid uptake of oxygen pulses on the BSCFO surface [33] possibly counterbalancing the more efficient oxygen release where MgO is present. On the other hand, using more homogeneous wash-coated samples where the BSCFO surface is completely shielded by MgO, the enhanced oxygen release rate yields a net improvement in permeation.

3.2.2. BSMFO membrane

The permeability of the BSMFO membrane modified via the sol-gel method was the same as for the bare membrane tested under equivalent conditions. Although an increase in permeability was observed depositing the catalyst by wash-coating, it did not allow oxygen permeability higher than 0.070 mL min⁻¹ cm⁻² at 1000 °C. Indeed, the low oxygen permeability observed with BSMFO modified membranes was due to the slow transport of oxygen anions through the bulk of the BSMFO membrane as explained before. Hence, the impact of the surface modification did not change the order of magnitude of the permeability obtained with the bare membrane.

3.3. Comparison of the catalytic performance of BSCFO and BSMFO membranes

OCM catalytic tests are summarized in Table 2. They refer only to the two modified membranes, BSCFO and BSMFO, which were stable enough under the operating conditions. As a matter of fact, although the BBFO membrane covered an interesting permeability window, the lack of stability of this

Table 2

Influence of oxygen supply on the OCM reaction in membrane reactors at 950 °C (CH₄ concentration: 10%/reactant flow rate: 85 mL min⁻¹)

Membranes		Catalytic results		
Type	Permeability (mL min ⁻¹ cm ⁻²)	Catalyst	CH ₄ conv. (%)	C ₂ select. (%)
BSCFO (bare)	1.92	–	4.3	5.6
BSCFO (gel)	2.06	2%-Pt/MgO	7.0	5.1
BSCFO (wash-coat)	4.35	2%-Pt/MgO	19.3	2.2
BSMFO (bare)	0.018	–	2.9	47
BSMFO (gel)	0.018	2%-Pt/MgO	6.6	46
BSMFO (wash-coat)	0.064	2%-Pt/MgO	3.5	0

membrane did not allow us to obtain performance data for a sufficient time span. This membrane may be reconsidered when more active catalyst would allow operation at lower temperature where the poor thermal stability does not present a significant issue.

3.3.1. BSCFO membranes

Surprisingly, a non-negligible amount of gaseous oxygen was found in the effluent of the reactant side for the sol–gel prepared BSCFO sample while this was not the case for the wash-coat modified one. The conversion of methane was higher with the wash-coated catalyst but selectivity was lower than the one obtained for the sol–gel catalyst (Fig. 7). The results obtained by Shao et al. [10] on a similar Ba_{0.5}Sr_{0.5}Co_{0.8}Fe_{0.2}O_{3-δ} membrane (CH₄ conversion: 3.4%, C₂ selectivity: 59.5% at $T = 900$ °C) were most probably due to the higher methane concentration in the feed (50%-CH₄/50%-He) used in that study. Experimental work in our laboratory (data not presented) indicated increasing C₂ selectivity with rising total flow rate of the reactant and methane concentration in the feed. This finding reflects at least partially the already mentioned general tendency of declining selectivity with rising conversion.

3.3.2. BSMFO membranes

The BSMFO membrane with sol–gel catalyst showed significantly better results (Fig. 8) with a C₂ selectivity of 46% and a CH₄ conversion of 6.6% (yield: 3%) at 950 °C. Here the C₂ selectivity is much higher than what could be observed for a BSCFO membrane exhibiting comparable methane

conversions under equivalent conditions. Nevertheless, no C₂ selectivity and poor methane conversion were found using the BSMFO modified by the wash-coating method. This behavior was very different from what was observed for the BSCFO based membranes. According to these results, the slow oxygen transport through the volume of the BSMFO membrane did not allow to obtain good performances at higher catalyst loading. This observation underlines the decisive role of a well balanced system offering just the right oxygen permeation flux for a given activity of the catalyst coating. Thus, the improved selectivity using a BSMFO membrane (prepared by sol–gel) could be correlated to the low quantity of Pt/MgO catalyst deposited on its surface, in line with the relatively limited oxygen permeation. In turn, the larger catalyst quantity obtained by wash-coating combined with a lack of available oxygen lead to a deactivation of the catalyst, most likely by extensive coking.

Nevertheless, both bare and sol–gel modified BSMFO membrane surfaces are much more sensitive to deep perovskite reduction leading finally to a structural destruction during long time-on-stream runs. Degradation proceeds in those cases much more rapidly compared to the membrane modified by wash-coating as this membrane takes probably benefit of the dense catalyst coating constituting a kind of protective layer. However, the presence of small defects in the wash-coated Pt/MgO layer should also lead to the observed slower alteration of the BSMFO surface during the reaction. As the BSCFO membrane is much more stable under our operating conditions, no surface change is observed during the reaction with or

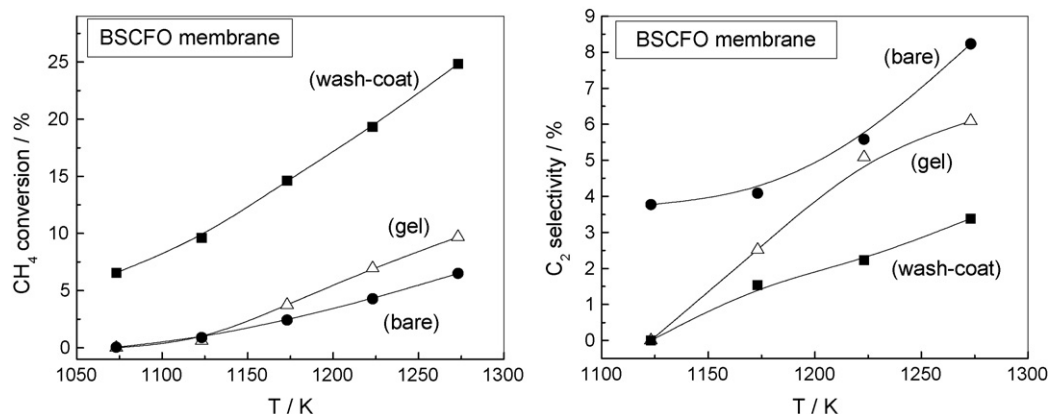


Fig. 7. Comparison of CH₄ conversion (left) and C₂ selectivity (right) for BSCFO based membranes at low CH₄ conc. in the reactant feed (CH₄ concentration: 10%/reactant flow rate: 85 mL min⁻¹).

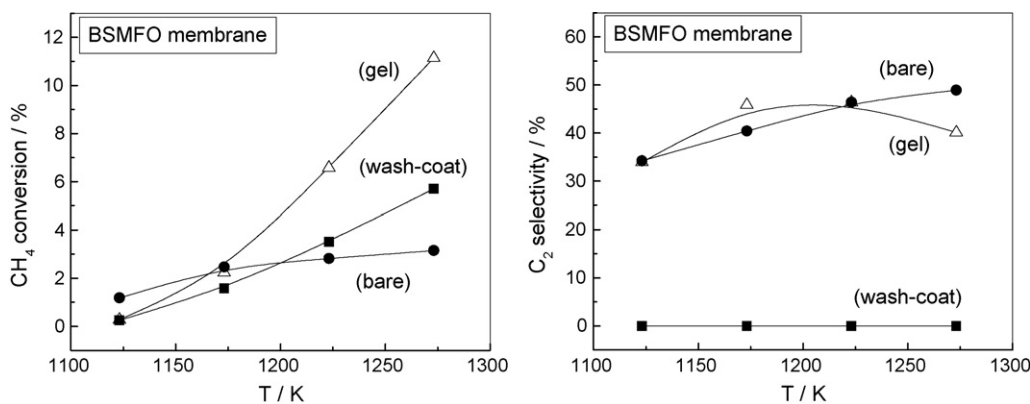


Fig. 8. Catalytic activity of the BSMFO membrane (CH₄ concentration: 10%/reactant flow rate: 85 mL min⁻¹).

without catalyst. Therefore, it appears that both elements of the catalytic membrane, base material and catalyst, are closely dependant from each other. Moreover, the role of the catalyst covering the whole membrane surface is not limited to methane activation but it allows additionally for higher oxygen permeability and a better protection of the membrane surface against perovskite reduction under reaction conditions when the perovskite structure is not directly in contact with methane.

Given the above outlined complexity of interactions between the surface catalyst and the oxygen supplying membrane, it seems indispensable to underline the general interest of the work benchmarking the reported membrane configuration against competing strategies previously reported in literature. First, it should be noted that there is no commercial process for the OCM, which could be related to high investment cost introducing commercially such a technology. In turn, C₂ productivity is a key element to evaluate different concepts, which can be used to compare the performance of the membrane reactor to conventional fixed bed reactor. The present membrane configuration allows a C₂ productivity (ethylene and ethane) of 6×10^{-5} mol(C₂)/(g_{cat} s) compared to 6×10^{-6} mol(C₂)/(g_{cat} s) as peak performance for a catalyst like 10% Li/MgO extensively described in literature, tested in a fixed bed reactor. For the latter value, a 10% Li/MgO catalyst was tested in our laboratory as reference in methane/oxygen co-feed mode and fixed bed configuration under sufficiently close conditions (6.7% methane, 3.4% oxygen, balance Ar, temperature range 600–800 °C). Besides the fact that the membrane reactor is obviously by far superior, an interesting fundamental aspect is revealed by the selective catalytic action of platinum. As a matter of fact, when used in the membrane configuration, a Pt based catalyst allows obtaining coupling products while usually only partial oxidation is observed for comparable noble metal based systems under fixed bed and co-feed configuration. Finally, it should be stressed that there are general benefits related to a membrane configuration such as (i) the dispense of pure oxygen feeds, (ii) an improved safety of operation as hydrocarbon/oxygen mixtures are avoided and finally and (iii) a higher productivity related to the fact that the global reactant ratio in a membrane reactor can be closer to stoichiometry than in a fixed bed reactor for flammability reasons.

On the other hand, the catalytic performance could currently be under evaluated as there are some drawbacks originating from the disk shape of the membrane considering the hydrodynamics of the reactor, such as dead volumes close to the outer alumina tube. Indeed, it would be desirable to evaluate the membrane reactor performance with tubular configurations. The reactor configuration in this work was chosen due to the ease of membrane preparation and the avoidance of a temperature profile over the membrane, thus allowing to measure specific catalyst activities (and therefore productivities) for comparison with fixed bed configuration.

One should note finally that in order to minimize the impact of hydrodynamics on the performance, the reactor depicted in Fig. 4 makes use of a plunger tube, extracting the effluent at the centre of the membrane disk very close (less than 1 mm) from the membrane surface. Furthermore, local reactant velocities were kept high, which is currently achieved by a rather high reactant flow rate. To the largest possible extent it was thus attempted to keep diffusion path lengths short and as uniform as possible.

4. Conclusion

In this study, the obvious difference in oxygen permeability between the tested membranes (BSCFO, BSMFO) allowed us comparing the OCM catalytic performance of the same catalyst at different oxygen supply rates. The impact of the oxygen supply on the performance of a Pt/MgO catalyst was demonstrated as an oxygen supply corresponding to the quantity needed by the catalyst should provide better C₂ selectivity and/or methane conversion. In fact, the formulation of the catalyst should be determined by the permeability of the membrane: a catalyst showing a high catalytic activity would be totally inefficient, and possibly even detrimental, when associated to a low permeable membrane. On the other hand, a highly permeable membrane requires a highly active catalyst to avoid poor C₂ selectivity. In that sense, the permeability of the membrane represents a key information to choose the right catalytic formulation once it is ensured that this formulation may be stably deposited at a suitable specific loading.

More specifically, it may be concluded that the most promising BSCFO membrane reactor suffers of decreased

selectivity as the oxygen supply rate is too high compared to the conversion rate for the given catalyst loading and conditions. Thus, aiming at stable reactors with high performance, enhancements in the catalytic activity are obviously required. Balancing the oxygen permeation with more advanced catalysts is required when passing to well performing membrane material like BSCFO, giving in this way access to better performing membrane reactors.

These results, especially when expressed in term of C_2 productivity, proved again the potential of catalytic dense membrane reactors in OCM justifying more investigations targeting at adherent and stable performing catalyst layers resisting to the severe OCM operating conditions.

Acknowledgements

Part of this work was supported by the European research project “TOPCOMBI” (contract NMP2-CT2005-515792). The authors gratefully acknowledge the workshop for electronics at IRCELYON for its technical support.

References

- [1] G.J. Tjatjopoulos, P.T. Ketekides, D.K. Iatrides, I.A. Vasalos, *Catal. Today* 21 (1994) 387.
- [2] Y. Lu, A.G. Dixon, W.R. Moser, Y.H. Ma, U. Balachandran, *J. Mem. Sci.* 170 (2000) 27.
- [3] Y. Amenoya, V.I. Birss, M. Golezdzinowski, M. Galuszka, A.R. Sanger, *Catal. Rev. Sci. Eng.* 32 (1990) 163.
- [4] Y.S. Lin, Y. Zeng, *J. Catal.* 164 (1996) 220.
- [5] S. Liu, X. Tan, K. Li, R. Hughes, *Catal. Rev.* 43 (2001) 147.
- [6] A.M. Ramachandra, Y. Lu, Y.H. Ma, W.R. Moser, A.G. Dixon, *J. Mem. Sci.* 116 (1996) 253.
- [7] Y. Lu, A.G. Dixon, W.R. Moser, Y.H. Ma, *Chem. Eng. Sci.* 55 (2000) 4901.
- [8] J. Han, Y. Zeng, Y.S. Lin, *J. Mem. Sci.* 132 (1997) 235.
- [9] J.E. ten Elshof, H.J.M. Bouwmeester, H. Verweij, *Appl. Catal. A: Gen.* 130 (1995) 195.
- [10] Z. Shao, H. Dong, G. Xiong, Y. Cong, W. Yang, *J. Mem. Sci.* 183 (2001) 181.
- [11] Y. Zeng, Y.S. Lin, S.L. Swartz, *J. Mem. Sci.* 150 (1998) 87.
- [12] F.T. Akin, Y.S. Lin, *AIChE J.* 48 (2002) 2298.
- [13] H. Wang, Y. Cong, W. Yang, *Catal. Today* 104 (2005) 160.
- [14] M. Rebeilleau-Dassonneville, S. Rosini, A.C. van Veen, D. Farrusseng, C. Mirodatos, *Catal. Today* 104 (2005) 131.
- [15] H. Lu, J. Tong, Z. Deng, Y. Cong, W. Yang, *Mater. Res. Bull.* 41 (2006) 683.
- [16] Y. Tereoka, H.-M. Zhang, K. Okamoto, N. Yamazoe, *Mater. Res. Bull.* 23 (1988) 51.
- [17] T.J. Maznec, T.L. Cable, J.G. Frye, *Solid State Ionics* 53–56 (1992) 111.
- [18] H. Kruidhof, H.J.M. Bouwmeester, R.H.E. van Doorn, A.J. Burggraaf, *Solid State Ionics* 63–65 (1993) 818.
- [19] S. Pei, M.S. Kleegfisch, C.A. Udovich, U. Balachandran, *Catal. Lett.* 30 (1995) 201.
- [20] V.V. Kharton, E.N. Naumovich, A.V. Nikolaev, *J. Mem. Sci.* 111–112 (1996) 149.
- [21] X.F. Zhu, H.H. Wang, W.S. Yang, *Chem. Commun.* 9 (2004) 1130.
- [22] Z. Shao, W. Yang, Y. Cong, H. Dong, J. Tong, G. Xiong, *J. Mem. Sci.* 172 (2000) 177.
- [23] Z. Shao, G. Xiong, H. Dong, W. Yang, L. Lin, *Sep. Purif. Technol.* 25 (2001) 97.
- [24] J. Caro, T. Schiestel, S. Werth, H. Wang, A. Kleinert, P. Kölsch, *Desalination* 199 (2006) 415.
- [25] H. Wang, C. Tablet, T. Schiestel, S. Werth, J. Caro, *Catal. Commun.* 7 (2006) 907.
- [26] Z. Shao, G. Xiong, J. Tong, H. Dong, W. Yang, *Sep. Purif. Technol.* 25 (2001) 419.
- [27] J.A. Roos, S.J. Korf, R.H.J. Veehof, J.G. van Ommen, J.R.H. Ross, *Appl. Catal.* 52 (1989) 147.
- [28] G.J. Tjatjopoulos, I.A. Vasalos, *Catal. Today* 13 (1992) 361.
- [29] J.H.B.J. Hoebink, P.M. Couwenberg, G.B. Marin, *Chem. Eng. Sci.* 49 (1994) 5453.
- [30] R.H. Nibbelke, J. Scheerova, M.H.J.M. de Croon, G.B. Marin, *J. Catal.* 156 (1995) 106.
- [31] V.A. Sadykov, T.G. Kuznetsova, Y.V. Frolova-Borchert, G.M. Alikina, A.I. Lukashevich, V.A. Rogov, V.S. Muzykantov, L.G. Pinaeva, E.M. Sadovskaya, Y.A. Ivanova, E.A. Paukshtis, N.V. Mezentseva, L.C. Batuev, V.N. Parmon, S. Neophytides, E. Kemnitz, K. Scheurell, C. Mirodatos, A.C. van Veen, *Catal. Today* 117 (2006) 475.
- [32] M. Salazar, D.A. Berry, T.H. Gardner, D. Shekhawat, D. Floyd, *Appl. Catal. A: Gen.* 310 (2006) 54.
- [33] A.C. van Veen, D. Farrusseng, M. Rebeilleau, T. Decamp, A. Holzwarth, Y. Schuurman, C. Mirodatos, *J. Catal.* 216 (2003) 135.